Cornell University

COMPUTER - AIDED ENGINEERING:

APPLICATIONS TO BIOLOGICAL PROCESS

BEE 4530

Murdering the Murder Hornet: Heat and CO_2 Exchange in a Bee-ball

A Report presented to the Course Staff of BEE 4530 / ENGRC 4530 at Cornell University in Partial Fulfillment of the Requirements for the classes.

May 14, 2021

Table of Contents

1 Executive Summary

Bee-balling is a defensive technique employed by Japanese honeybees, Apis cerana japonica, against the predatory Asian giant hornet, Vespa mandarinia. Upon recognition of the hornet intruder within the hive, hundreds of honeybees surround and restrain the hornet; forming a bee-ball. Subsequently the bee-ball experiences three distinct phases of temperature change (heating, heat retaining, and break up). The bees simultaneously elevate CO_2 levels and temperature within the bee-ball, which jointly act to kill the hornet. To gain an improved mechanistic understanding of this process, a computational model of heat transfer and carbon dioxide transfer specifically examining the heating and heat retaining phase within the bee-ball was developed. The manipulation of model parameters to simulate different environmental conditions, bee arrangement and production rates provides insight into the process that would otherwise be difficult or near impossible to obtain through pure experimentation.

In this study, we considered the honeybees and the hornet to generate heat and CO_2, while also exchanging heat to each other, and losing CO_2 to the surroundings. To investigate the mechanism of the bee-balling behavior, we used COMSOL, a multiphysics finite element analysis and simulation software, to develop a simple geometry and replicate the heat and CO_2 exchanging properties of the honeybees and the hornet during heating and heat retaining phase of the bee-balling process. The results of this study provide insight behind why bee-balls form, how the honeybees utilize heat and CO_2 and modulate their movement, heat and CO_2 production rate to effectively murder the murder hornet.

Keywords: Heating Bee-ball, Heat Transfer, CO_2 Mass Transfer, Honeybee and Hornet, Computational Solution

2 Introduction

Japanese honeybees, *Apis cerana japonica*, are endothermic insects living in colonies with a complicated social organization (Stabentheiner et al., 2007). Their colonies contain food stores in the form of honey and pollen, as well as the brood, the queen and the bees themselves (Nouvian et al., 2016). As a result, it is imperative that colonies formulate a strong social defense against predators, who seek to steal honey or prey on the bees and their brood (Stabentheiner et al., 2007). One especially deadly natural enemy that threatens Japanese honeybees is the Asian Giant Hornet, also known as Vespa *mandarinia* (Ono et al., 1987).

To the casual observer, honeybees and hornets may appear similar, but they are in fact bitter adversaries. While both species may live socially, hornets produce no honey and instead must hunt to feed (Stabentheiner et al., 2007). For the honeybees, this means they must remain on high alert for hornet scouts given that they are at an inherent disadvantage defending against the hornet. The honeybees are a 1/5 of the size of the hornet, and their stingers are rendered useless against the thick impenetrable hornet cuticle (Matsuura & Sakagami). Thus, although a bees' most notable defense is their sting, the bees must employ a different defense tactic.

While a single hornet scout may not initially kill the honeybees, it will mark the hive, allowing it to find it again once it returns to its own hive to notify its queen and other members (Matsuura & Sakagami). Should it return later with a larger party of hornets, they will easily slaughter, via decapitation, the entire hive in under an hour (Matsuura & Sakagami). To protect the hive from massacre it is critical the scout never marks the hive, thus demanding a drastic and rapid defensive response from the bees.

Due to high predatory pressure, the Japanese honeybees have perfected a particular defense mechanism to a degree that no other in its species can execute with the same level of efficiency: bee-balling (Stabentheiner et al., 2007). The process was observed to consist of three rough stages: consisting of 1) the max hornet temperature increase from ambient to 46°C, 2) temperature maintenance for 20 minutes, and 3) temperature drop back to ambient (Ono et al., 1987). Later, these stages were termed heating phase, heat-retaining phase, and breakup phase with peak temperatures occurring at the end of the heating phase (Hosono et al., 2017).

When a hornet scout is detected within the hive by guards, an alarm is sent out to the workers in the hive.Within seconds of recognition, the hornet is engulfed by hundreds of bees in a densely packed bee-ball and restrained against the ground of the hive (Hosono et al., 2017). The Japanese honeybees make no attempts to sting the hornet – a waste of energy as the cuticle is too thick (Hosono et al., 2017). Instead, the bees raise the internal temperature of the bee-ball through vibration of their flight muscles.The bees closest to the hornet have been observed to heat the strongest, while surrounding bees demonstrate lower activity and produce less heat

(Stabentheiner et al., 2007). Nevertheless, they still play an important role in the bee-balling process. The tight packing and limited movement of these bees are speculated to function as a layer of insulation and reduce convection (Stabentheiner et al. 2007). When close together, the bee's setae (hairs) interlock, limiting air movement and decreasing overall thermal conductivity (Southwick, 1985).

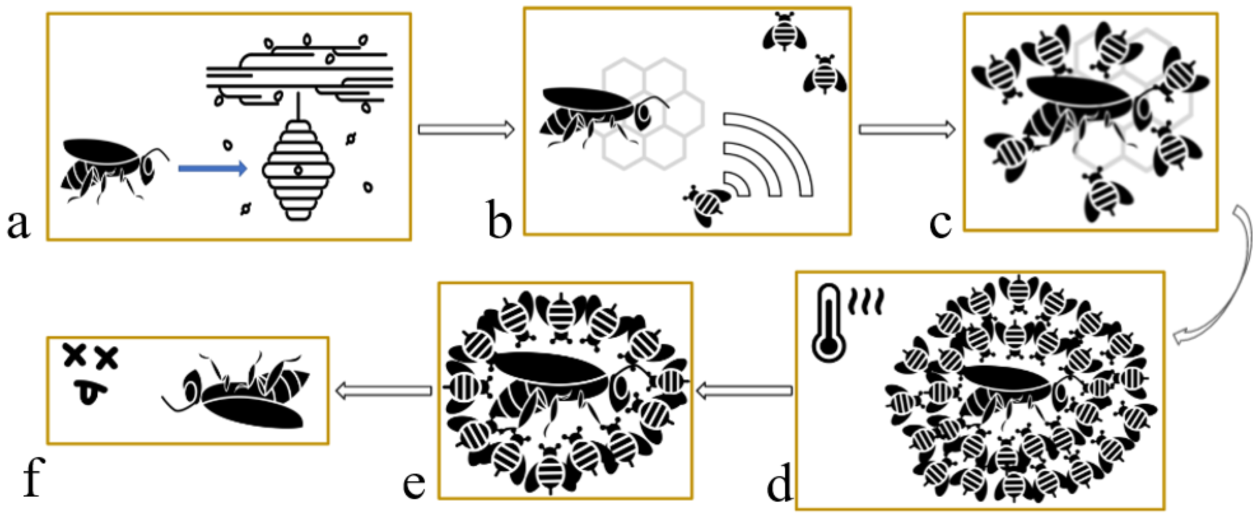

Figure 1: Stages of bee-balling. a) Hornet entry into beehive. b) Recognition of the hornet and sounding of an alarm. c) Bee-ball formation begins. d) Bees raise and maintain temperature during heating and heat-retaining phase. e) Bees begin to disband during the breakup phase. f) Bee-ball fully disbanded, leaving the dead hornet.

Heat is also generated by the hornet itself as it struggles against the bees (Hosono et al., 2017). While restrained by the bees in the bee-ball with minimal air flow, the hornet begins to overheat (Hosono et al., 2017). Simultaneously, the bees are also raising the internal CO_2 level within the bee-ball (Sugahara et al., 2012). Coinciding with the high rates of metabolism is elevated respiration. This combined with the dense packing of the bee-ball inhibiting air flow, the CO_2 in the bee's expiratory air begins to rise (Sugahara et al., 2012). The elevated CO_2 within the microenvironment of the bee-ball acts to lower the hornet's thermal tolerance and is critical to the success of the process (Sugahara et al., 2012). In studies where hornets were placed incubators at temperatures found to be lethal within bee-balls, no death occurred (Hosono et al., 2017); however when exposed to concentrations of CO_2 in expiratory air lethal temperature was lowered by 2°C (Sugahara et al., 2012). Thus, within roughly 10 minutes the temperature of the thermal ball exceeds the lowest thermal tolerance of the hornet ~46°C but below the lethal thermal limit of the bees themselves (Hosono et al., 2017). Subsequently, this temperature is maintained for approximately 20 minutes longer to ensure that the trapped hornet dies before the ball breaks in the heat retaining phase (Hosono et al., 2017). Finally, in the break up phase, around 30 minutes after the initial formation, the bees begin to disperse leaving a dead hornet; thus, the hornet is killed jointly via overheating and asphyxiation (Hosono et al., 2017).

The Japanese honeybees bee-balling behavior is in some aspects simply an extreme case of other bee thermoregulatory behaviors, chiefly winter clustering. Bees do not hibernate over winter; thus, they must avoid freezing in an efficient way so as to avoid prematurely depleting honey stores (Southwick, 1985). To accomplish this, the entire hive clusters together in a large dense mass. The bees closest to the center form the core of the cluster and produce the most heat similar to the behavior displayed in the bee-ball via shivering thermogenesis (Ken et al., 2005; Southwick, 1985). Furthermore, similar to a bee-ball, the peripheral bees surrounding the core, the mantle bees, act as an insulating layer (Southwick, 1985). However, a clear distinction between winter clustering and bee-balling is the duration. Given that the winter clusters are maintained for a significantly longer period of time and efficiency is key for survival – not temperature maximization at the core-bees in winter clusters display several behaviors not observed in bee-balls (Southwick, 1985). One is that the bees continuously circulate through the ball to ensure that the bees on the periphery are not exposed to freezing temperatures for an extended period of time — in a way analogous to convection currents within the ball; another is the internal temperature of the cluster is maintained at a lower, more comfortable 35°C (Southwick, 1985). Studies of swarms make note of the same mantle and core organization of bees; however, in the same fashion that winter clusters differ, the swarms also have significantly more participants than bee-balls, circulation of the bees occurs and a lower internal temp is maintained (Heinrich, 1981).

Given these critical differences between winter clustering and bee-balling, the findings are not implicitly applicable, leaving questions about how exactly bee-balls are able to achieve and maintain such high temperatures and concentrations of CO_2. Furthermore, due to difficulties in monitoring and measuring the honeybee and hornet temperatures in a natural setting without disturbing the physical process, most studies on the bee-balling process were either mostly observational or under experimental settings where the process is disturbed to make measurement possible, providing only approximate temperature and CO_2 profiles for the hornet and the honeybees during the bee-balling process (Hosono et al., 2017; Sugahara et al., 2012). While a numerical model approach is not common in bee studies, numerical models would be an effective viable alternative to investigate and approximate the physics of heat and CO_2 transfer during the bee-balling process under natural conditions, providing a more cohesive picture of the process.

This study explores the heat and CO_2 transport process in bee-balling through COMSOL, focusing on the heating phase and the heat-retaining phase, modeling how honeybees rapidly raise temperature and kill the hornet. The break-up phase is currently not discussed in this study since the hornet has been killed at the end of the heating phase as well as the heat-retaining phase (Sugahara & Sakamoto, 2009)

2.1 Problem Statement and Design Objectives

We aim to build a computational model of a bee-ball under natural conditions, to gain a better mechanistic understanding of the process by exploring the following:

1. The temperature profile of the honeybee bee-balling process under natural conditions

2. The effect of different environment conditions on the bee-balling process

3. The effect of bee arrangement in the bee-ball (including honeybee layer thickness, density and heat conductivity) on the bee-balling process

4. The effect of different heat production rate and CO_2 production rate of the honeybee and the hornet on the bee-balling process

3 Methods

3.1 Schematic

The model's schematic sought to capture the relevant geometric aspects of a naturally formed bee-ball. Naturally formed bee-balls take place overtop comb within the hive, thus the comb is included underneath the bee-ball itself within the domain. Within the honeybees within the bee-ball are divided into two separate groups, this is reflected in the geometry assuming:

1) Bee-balls use the same organizational pattern as other similar endothermic heating processes bees employ. The bee's metabolism at the core is higher than those towards the periphery in the mantle

The bee-ball was simplified to a two dimensional geometry consisting of three solid regions: hornet, active bee and passive bee regions. Underlying the simplification of the bee-ball's three-dimensional ellipsoid geometry to its two dimensional cross section were the following assumptions:

2) Negligible transport is present at the ends of the bee-ball (z-direction)

3) The hornet's body shape may be approximated as a cylinder (Figure 2)

4) Bee-ball is of uniform diameter along its entire length

The active bee and passive bee regions of the bee-ball are a composition of honeybees and air. However given the minimal air space between honeybees within the densely packed conditions of the bee-ball the geometry was modified under the assumption:

5) Air and honeybees in the active and passives bee layers are effectively solid

Furthermore given the limited availability of parameter data and knowledge concerning variation of the material properties within each region of the domain for the purposes of this model we assumed:

6) c_p, k, ρ, and D are constant within each region of the domain

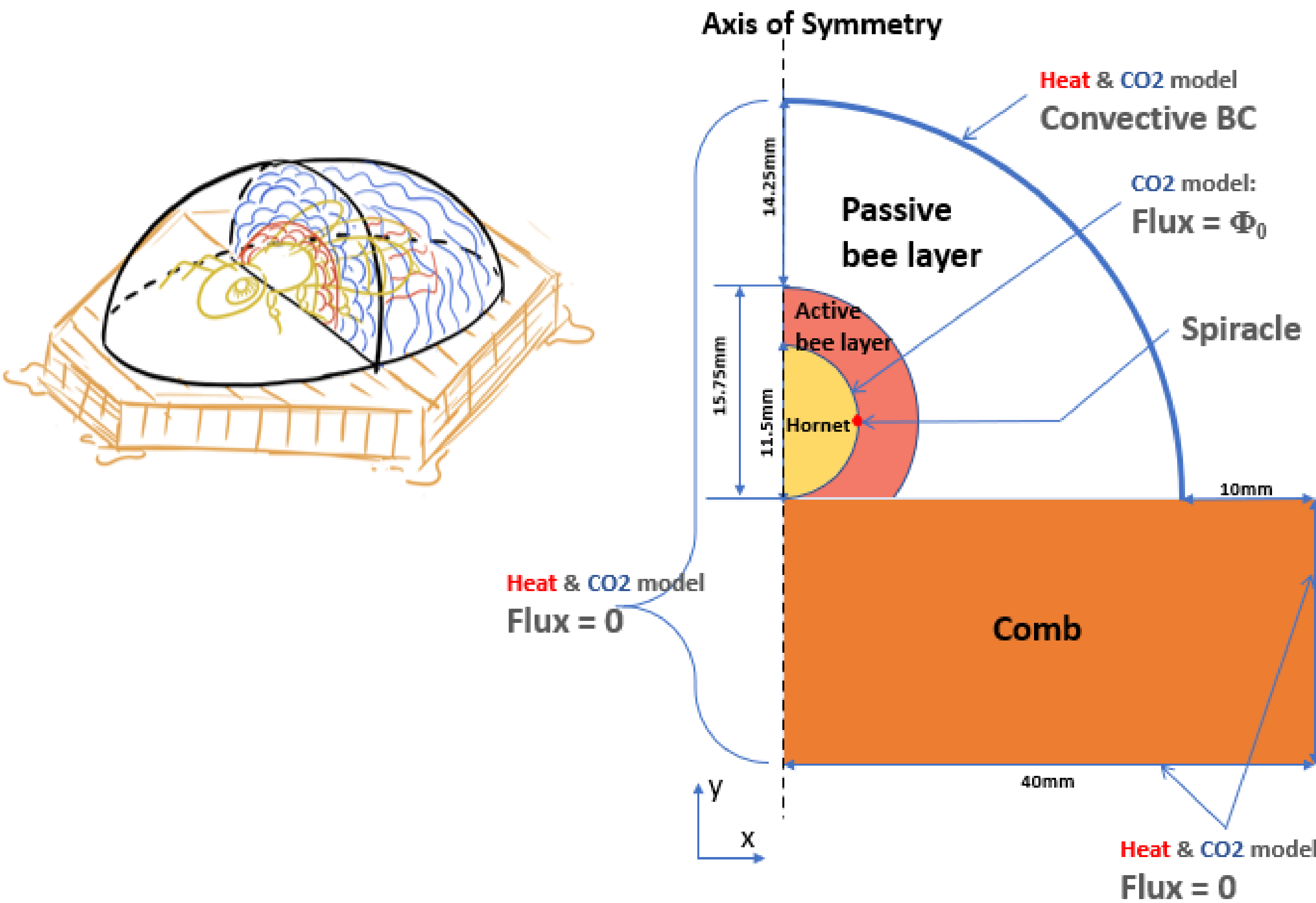

Figure 2: 2D geometry of the model in the Cartesian coordinates with dimensions. The hornet lies in the center of the honeybee-ball, and its body is highlighted with yellow. The spiracle of the hornet has been marked at the surface of it as a red point. The honeybee layer is made of the active bee layer (red) tightly wrapping the hornet as well as the passive bee layer on the outermost. The comb underneath the bee-ball is highlighted with orange. For both heat transfer and CO_2 mass transfer, convective boundary conditions (convective BC) at passive bee layer/ambient air interface, and flux = 0 at the distance (x = 40 mm, y = -20mm) sufficiently far into the comb from the bee-ball are applied. Flux= Φ_0 applies for CO_2 mass transfer at the hornet/active bee layer interface.

3.2 Parameters

All relevant parameters to heat and CO_2 transfer within the bee-ball were obtained from experimental data found in literature or the authors' own calculations. The values, relevant assumptions, calculations and sources are all found in the Appendix, Table A1.

3.3 Governing Equations

The relevant physics describing heat and CO_2 transfer within a bee-ball were modeled using the heat equation and mass transfer equation:

3.3.1 Heat Transfer

Heat Equation: $$\rho c_p \left(\underbrace{\frac{\partial T}{\partial t}}_{\text{transient}} + \cancel{\underbrace{u_x \frac{\partial T}{\partial x} + u_y \frac{\partial T}{\partial y}}} \right) = \underbrace{k \left(\frac{\partial^2 T}{\partial x^2} + \frac{\partial^2 T}{\partial y^2} \right)}_{\text{conduction}} + \underbrace{q}_{\text{generation}} \tag{1}$$

The transient, conduction, and generation terms were retained as shown in Equation 1. Heat generation varies between the different groups of participants within the bee-ball (hornet, active honeybees and passive honeybees) thus the generation term q varies with respect to position and temperature (due to temperature dependent changes in metabolism). The convection term was omitted under the assumption that bulk flow was negligible under tightly packed conditions of the bee-ball.

3.3.2 CO_2 Mass Transfer

Mass Equation: $$\underbrace{\frac{\partial c_A}{\partial t}}_{\text{transient}} + \cancel{\underbrace{u_x \frac{\partial c_A}{\partial x} + u_y \frac{\partial c_A}{\partial y}}_{\text{convection}}} = \underbrace{D_A \left(\frac{\partial^2 c_A}{\partial x^2} + \frac{\partial^2 c_A}{\partial y^2} \right)}_{\text{diffusion}} + \underbrace{R_A}_{\text{reaction}} \tag{2}$$

The transient, diffusion and reaction terms are retained as shown in Equation 2. Similarly, the reaction term R_A varies with respect to position and temperature within the domain but will be independent of concentration of CO_2. The convection term was omitted, with an assumption that there is no flow through the bee-ball.

3.4 Boundary and Initial Conditions

The model sought to simulate a bee-ball formed under natural conditions overtop honeycomb. As such the boundary and initial conditions were set to mimic the environment within a honeybee hive, the honeybees and the hornet.

3.4.1 Heat Transfer

Boundary Conditions:

1. At the interface of honeybee layer surface and surrounding air:

$$\vec{n} \cdot -k\nabla T = h(T - T_{\infty})$$

2. At the interface between comb and surrounding air:

$$\vec{n} \cdot -k\nabla T = h(T - T_{\infty})$$

3. At the distance (x = 40 mm, y = -20mm) sufficiently far into the comb from the bee-ball that heat transfer from bee-ball to this boundary will have negligible effect:

$$T|_{x=40, y=-20} = T_{comb}$$

Initial Conditions:

1. Initial temperature of the hornet:

$$T|_{t=0,\, hornet} = 36.69°C$$

2. Initial temperature of the honeybees (active and passive):

$$T|_{t=0,\, honeybee} = 39.55°C$$

3.4.2 CO_2 Mass Transfer

Boundary Conditions

1. At the interface of honeybee layer surface and surrounding air:

$$\vec{n} \cdot -D\nabla c = h_m(c_{surface} - c_{\infty})$$

2. At the interface of comb layer surface and surrounding air:

$$\vec{n} \cdot -D\nabla c = h_m(c_{surface} - c_{\infty})$$

3. At the interface of hornet and honeybee layer:

Φ = constant flux

4. At a distance (x = 40mm, y = -20mm) sufficiently far from the bee-ball into the comb, the mass transfer from the bee-ball will have negligible effect, thus the fluxes at this two boundaries are:

$$\Phi|_{x=40,y=-20} = 0$$

Initial Conditions

1. Initial CO_2 concentration in comb:
   $C_{comb} = c_{b,c}$
2. At the interface of comb layer surface and surrounding air:
   constant CO_2 concentration: $C|_{40<x<50} = C_{air}$\

3.5 Mesh

3.5.1 Mesh Convergence

A mesh convergence analysis was performed at the point (0.0025, 0.00575) in the model by determining the number of edge elements required for the temperature change at this point to change the least between simulations, ideally remaining constant. Figure 3 illustrates the mesh convergence result over a 30 min time range as shown below. As seen in Figure 3(b), the mesh convergence showed that all of the temperature profile lines converged together except for the line with a number of elements of 251; temperature profile lines for the number of elements of 8435, 3153, 679 showed very small difference and well convergence. Hence, the number of elements of 679 is chosen for the mesh of the model as going higher than that only increases computational time and memory.

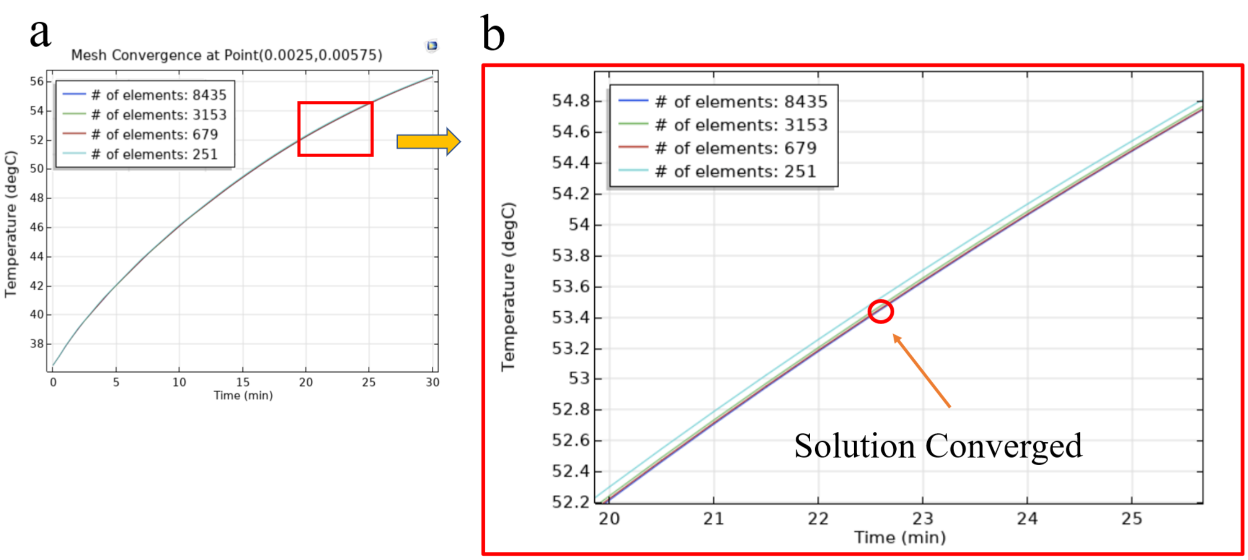

Figure 3. (a) mesh convergence graph of the model in the honeybee & hornet area for different numbers of elements ranging from 8435, 3153, 679, and 252 at the point (0.0025,0.00575); (b) enlarged view

3.5.2 Mesh

For the computational model of the bee-balling process in COMSOL, 679 number of elements was chosen for the model as determined from mesh convergence, constructed using free triangular elements for the honeybee and hornet section and mapped rectangle for the comb section as shown in Figure 4.

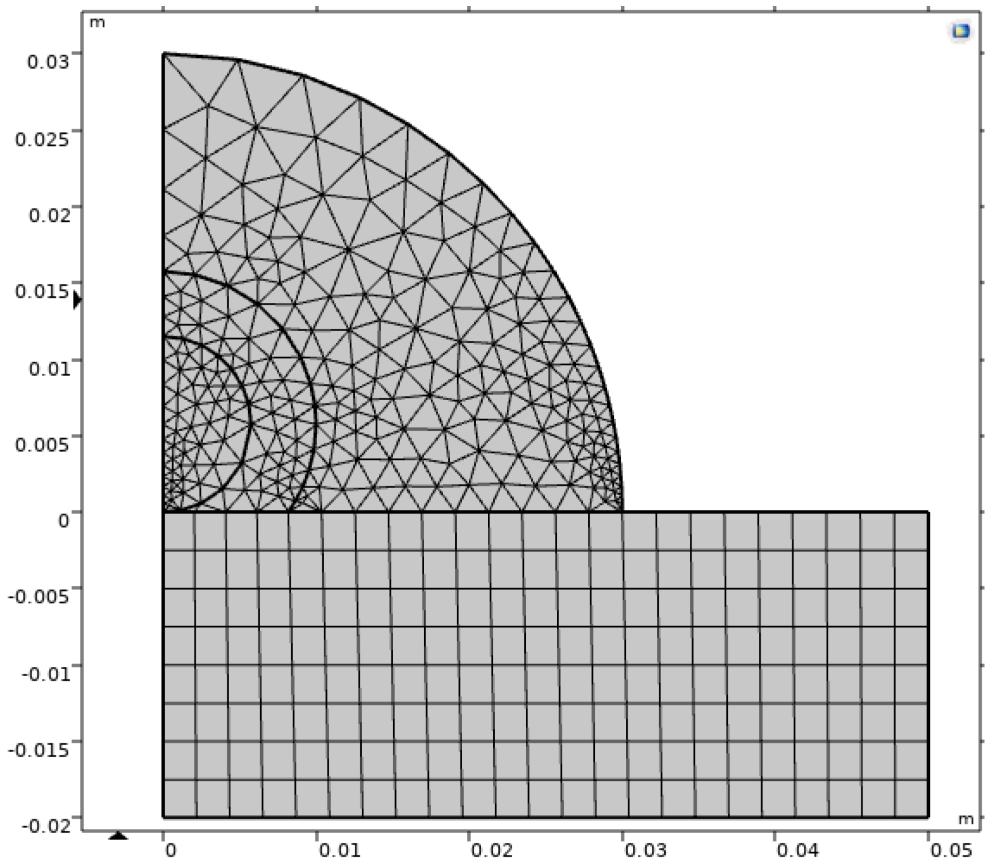

Figure 4: Mesh for the model generated in COMSOL. The maximum element size is 0.00296m and the minimum element size is 0.00001m with a maximum element growth rate of 1.25. The curvature factor is 0.25 and the resolution of narrow regions is 1. The total number of elements is 679, which was chosen as a result of the results of mesh convergence.

5 Solutions

5.1 Heat Transfer

The 30 minute span of the model encompasses two distinct phases of bee-balling. The first 10 minutes, referred to as the heating phase, is characterized by a steep increase in the temperature. The second phase which is approximately 20 minutes in duration is when the ball assumes a ‘steady state’ lethal temperature.

To assess the effectiveness of a bee-ball the hornet’s internal thoracic temperature and the inner bee-ball temperature are of primary interest. To model these respective temperature profiles, two points within the bee-ball were selected: the center of the hornet and a point within the active honeybee layer. Using the mesh discussed in section 4 and parameters as shown in Table A1, the following results were obtained:

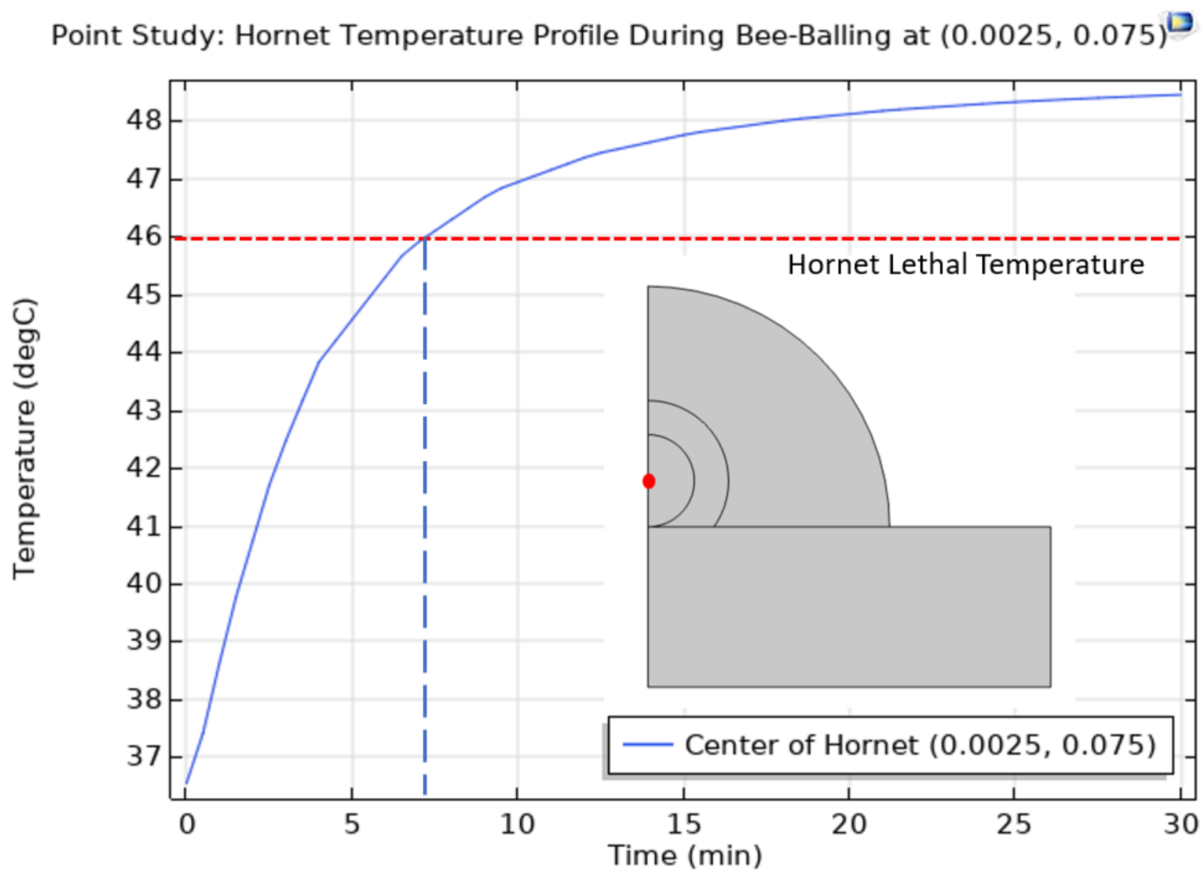

Figure 5: Temperature profile of the hornet center, point (0.0025, 0.075).

The greatest temperature change at the center of the hornet occurred during the first 10 minutes of bee-balling, increasing from 37°C to 47°C. Lethal temperature of the hornet center was reached at approximately 7 minutes. Over the remaining 20 minutes, the rate of temperature increased drastically declined, approaching a steady state temperature of approximately 48.5°C. This is consistent with the expectation that two distinct phases would develop in the temperature profile. By rapidly ramping the hornet's internal thoracic temperature to the lethal limit of 46°C within the heating phase and subsequently maintaining that temperature in excess, the model embodies the characteristic of a successful bee-ball.

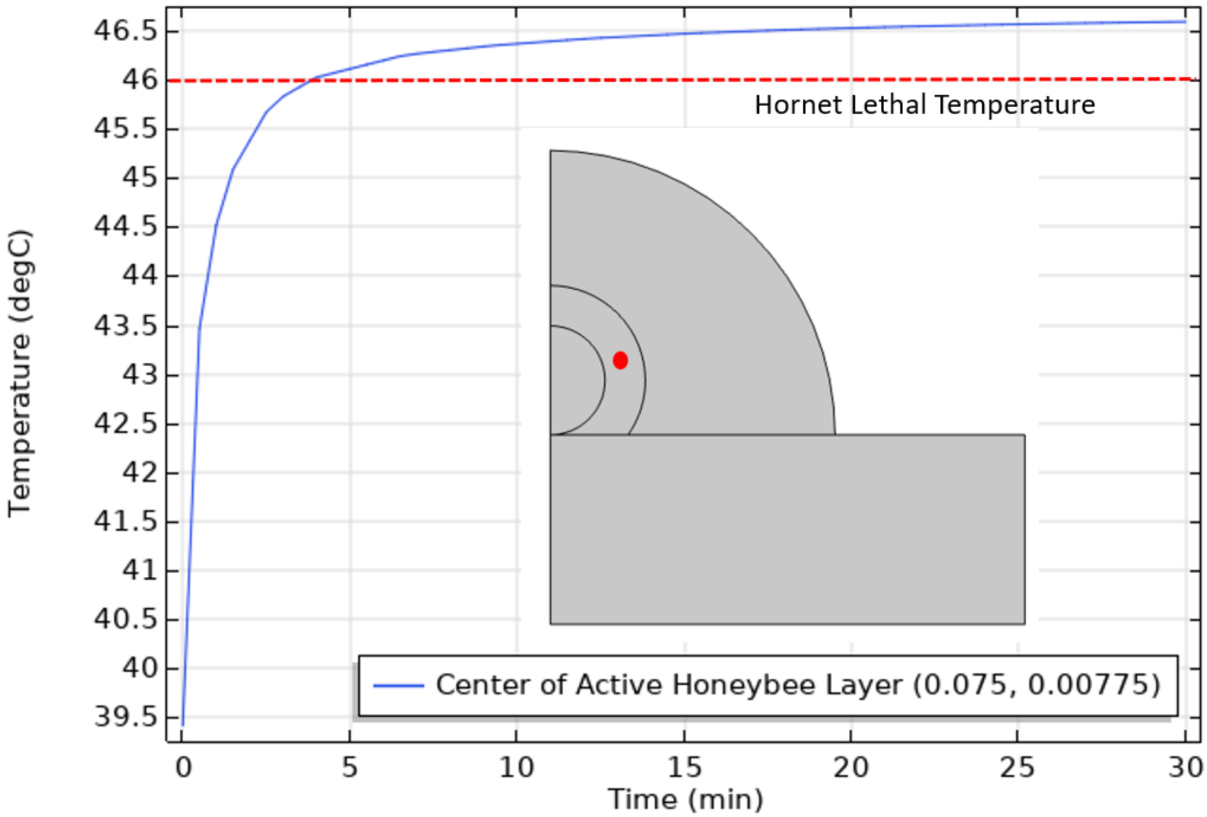

Figure 6: Temperature profile of active honeybee layer at point (0.0025, 0.075)

The most rapid temperature change within the active honeybee layer occurred within the first four minutes of bee-balling, increasing from 39.5°C to 46°C. Over the remaining model run time, the rate of temperature change significantly decreased such that it approached a steady state temperature of approximately 46.5°C. The bee-ball temperature never approaches the bee's lethal temperature of 50°C.

Similar to that of the hornet, this point complied with the expectation that two distinct phases of temperature would emerge. The honeybee temperature profile however transitioned to the next phase six minutes earlier than the hornet and approached a steady state temperature 2°C lower than the hornet. 30 minutes after the start of the process, the average temperature of the entire bee-ball was 34°C with the highest temperatures of the bee-ball concentrated towards the center in the hornet and active honeybees reside and lowest temperature concentrated towards the periphery of the bee-ball. The average temperature within the hornet and active bee region was 45°C with a maximum temperature of 47.8°C located within the hornet region. Meanwhile the average temperature of the passive honeybee layer was 32°C, a 13°C difference. Minimal heat penetration was determined to have occured into the honeycomb underneath the bee-ball.

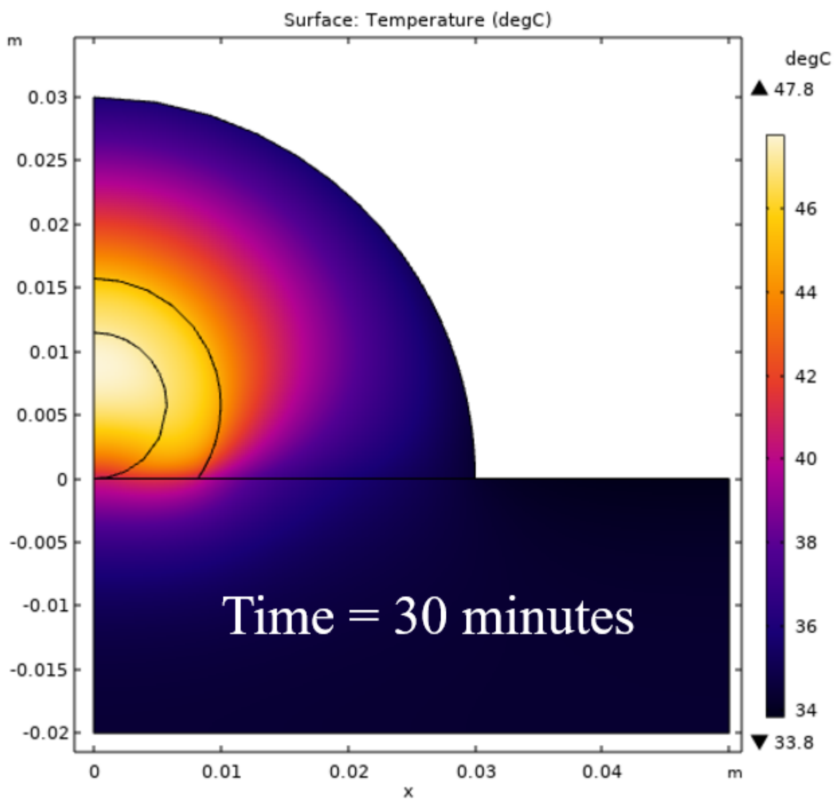

Figure 7: Surface plot of the bee-ball and the comb at 30 minutes.

The maximum bee-ball temperature of 47.8°C was located within the central region encompassing the hornet and active honeybees. Temperature increases from 36°C (blue) at the outermost passive honeybee layer boundary to 47.8°C(white) at the center of the hornet. Minimal heat penetration occurred into the comb beneath (-0.005m) the bee-ball.

5.2 CO_2 Mass Transfer

The CO_2 transport modeling primarily focuses on CO_2 diffusion through the air space in between the hornet and the honeybees, assuming no CO_2 accumulation inside and through their bodies.

To assess the CO_2 concentration in the bee-ball, a point nearby the hornet's spiracle was selected as our point of interest for this study as the hornet will be breathing in the surrounding air from its spiracle. Using the mesh discussed in section 4 and parameters as shown in Table A1, the following results were obtained:

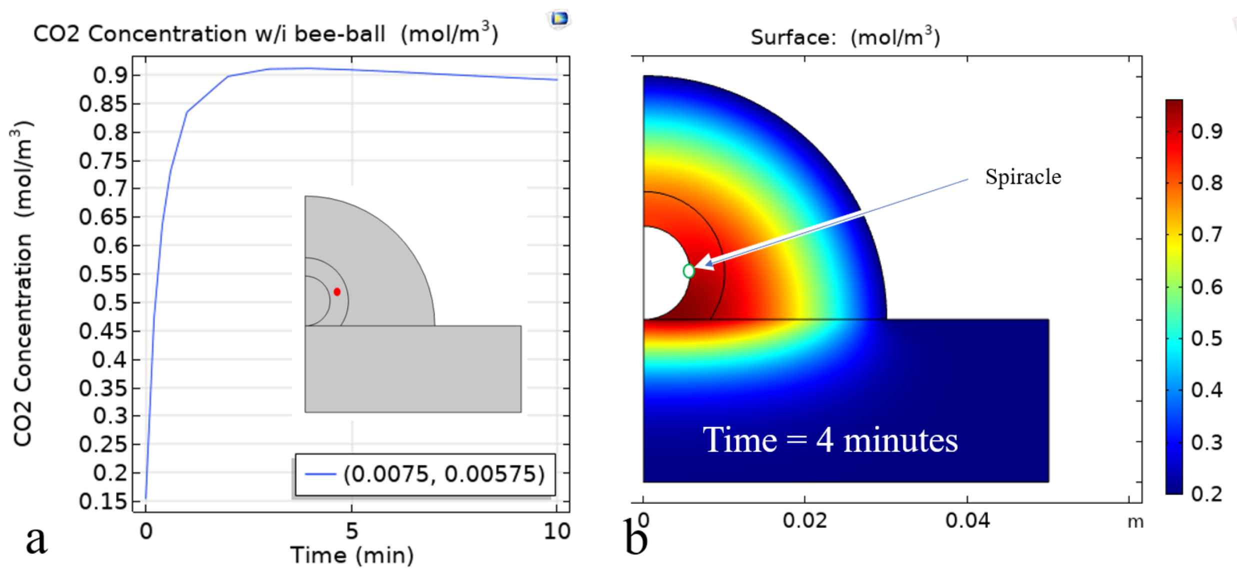

Figure 8: a) CO_2 concentration over 10 minutes at hornet's spiracle, point (0.0075,0.00575); b) Surface plot at 4 minutes of CO_2 concentration

Within the first four minutes, the CO_2 concentration sharply increases within the air that the hornet inhales, reaching a maximum concentration of approximately six times greater than levels found in ambient air. The region of highest CO_2 concentration at four minutes is concentrated in the air surrounding the spiracule. After reaching peak CO_2 concentration a gradual decline in CO_2 concentration is observed for the remainder of the time period under study. This coincided with hornet death (the model considers death to occur immediately upon exceeding the lethal temperature, of 46°C) and thus also cessation of the contribution of CO_2 from the hornet itself.

6 Validation

6.1 Heat Transfer Validation

6.1.1 Validation with Experimental Data

To validate the heat transfer model of the bee-ball, temperature profiles at the hornet center and inner bee-ball were compared to experimental data from Hosono et al. (2017). The methods employed to collect the experimental data were as follows. A live hornet was mounted on a temperature probe and presented at the entrance of a langstroth beehive, thus 'artificially' triggering bee-ball formation. The temperature of the internal thorax was recorded by a temperature probe previously inserted into the dorsal plate and the internal bee-ball temperature was recorded via the second temperature probe the hornet was immobilized upon (Hosono et al., 2017).

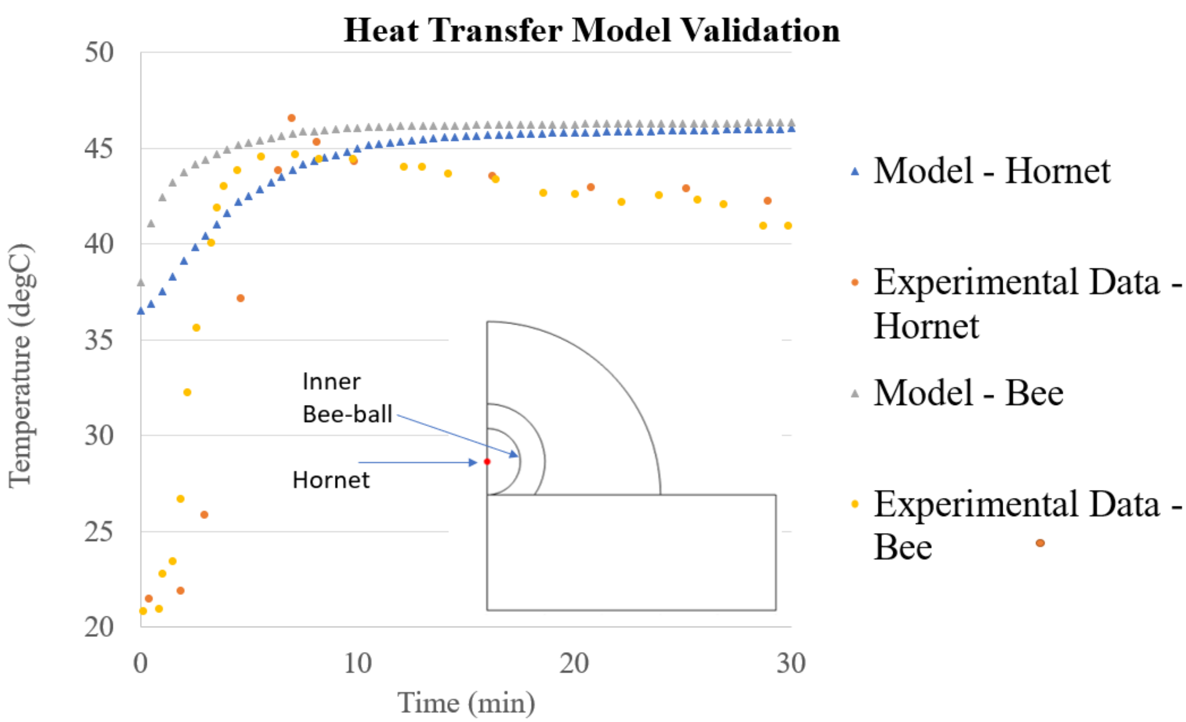

Figure 9: Honeybee internal temperature and hornet thoracic temperature validation. Blue triangles indicate temperature fluctuation of internal hornet thoracic from the model. Orange circles indicate hornet temperature fluctuation of internal hornet thoracic from Hosono et al., 2017. Gray triangles indicate temperature fluctuation of internal honeybee from the model. Yellow circles indicate hornet temperature fluctuation of internal honeybee thoracic from Hosono et al., 2017.

Both the temperature profiles (at the hornet center and internal bee-ball edge) generated by the model reflect the rapid temperature ramp from 0 - 10 minutes, followed by a sudden plateauing of temperature from 10 - 30 minutes observed during the heating and heat retention phase respectively in the experimental data. Overall, the model and experimental data trend similarly however there were several key differences observed. Whereas the model's temperature plateaus, signalling the start of the heat retention phase, a slow yet non negligible decrease in temperature was observed in the experimental heat retaining phase (10 minute to 30 min). This difference may be due to the disbandment of the bee-ball by some of the bees as time passes. A smaller number of bees in the bee-ball would ultimately lead to less heat production from the bee-ball layers overall in addition to a thinner layer of bees acting as an insulative layer. Given that our model was formulated under the assumption that the number of bees (and thus geometry) remains constant throughout the entire time period, temperature variation due to bees leaving the ball would not be captured. In addition, whereas the bee temperature profile in the model bee-ball is always higher than the temperature profile at the center of the hornet, the contrary is true for the temperature profiles recorded in the experimental bee-ball.

6.1.2 The Effect of Different Scenarios on Heat Transfer

Several notable differences should be acknowledged between the conditions under which the experimental data was collected and those assumed inof the model:

1) Lethal temperature: A range of temperatures over which hornets have been reported to be killed in the literature from 44 - 48°C (Hosono et al., 2017).

2) Control of heat production rate: The logic governing the bees' modulation of heat production as the bee-ball's temperature approaches lethal temperature to avoid overheating themselves is not thoroughly understood. Additionally, the assignment of bees to take on either the active vs. passive level of heating remains largely uncertain.

3) Ambient air temperature: The bee-balls from which temperature measurements were taken in this and other studies required the researchers to prompt the formation of the ball outside of the hive environment, whereas naturally occurring bee-balls occur exclusively within the hive. Our model seeks to portray a natural bee-balling behavior, hence the ambient air temperature (the internal hive temperature) employed in our model differs significantly from that of the experimental data.

These uncertainties prompted us to investigate by running our model through several scenarios to determine the effect of each of these on our results. Figures 10 and 11 show the results of running the following different scenarios through our models. Variations of different scenarios are described in Table 1 below.

Table 1: Description of various scenarios explored to determine their effects on our result

Scenario 0	**Current formulation**: hornet lethal temperature at 46°C, ambient temperature at 32.75°C
Scenario 1	**Decreasing lethal temperature to 44°C**, the lowest reported in the literature. The hornet heat production rate and the honeybee heat production rate are adjusted (the hornet stops producing heat and honeybee switches to passive heating at lethal temperature) to reflect the change in lethal temperature.
Scenario 2	The **thickness of the active bee layer is doubled**, the fraction of active bees to passive bees exceeds current ratio such that a majority of the bee-ball is takes on a heating role instead of insulative
Scenario 3	The outside **ambient temperature is adjusted to 18.5°C** to reflect the ambient temperature under a cooler environment
Scenario 4	**Active honeybee's heat production rate is modified** so that the honeybees transition from active to passive heat production rate in a piecewise cubic manner, instead of linearly as it is in the current formulation.
Scenario 5	**Initial temperature decreased to the initial temperature observed in the experiment.** Previously there was a ~20°C difference
Scenario 6	CO_2 flux of hornet is 0 after 4 min and honeybees CO_2 production rate returns to the rate under temperature (30°C), approximately half of its CO_2 production rate under max temperature

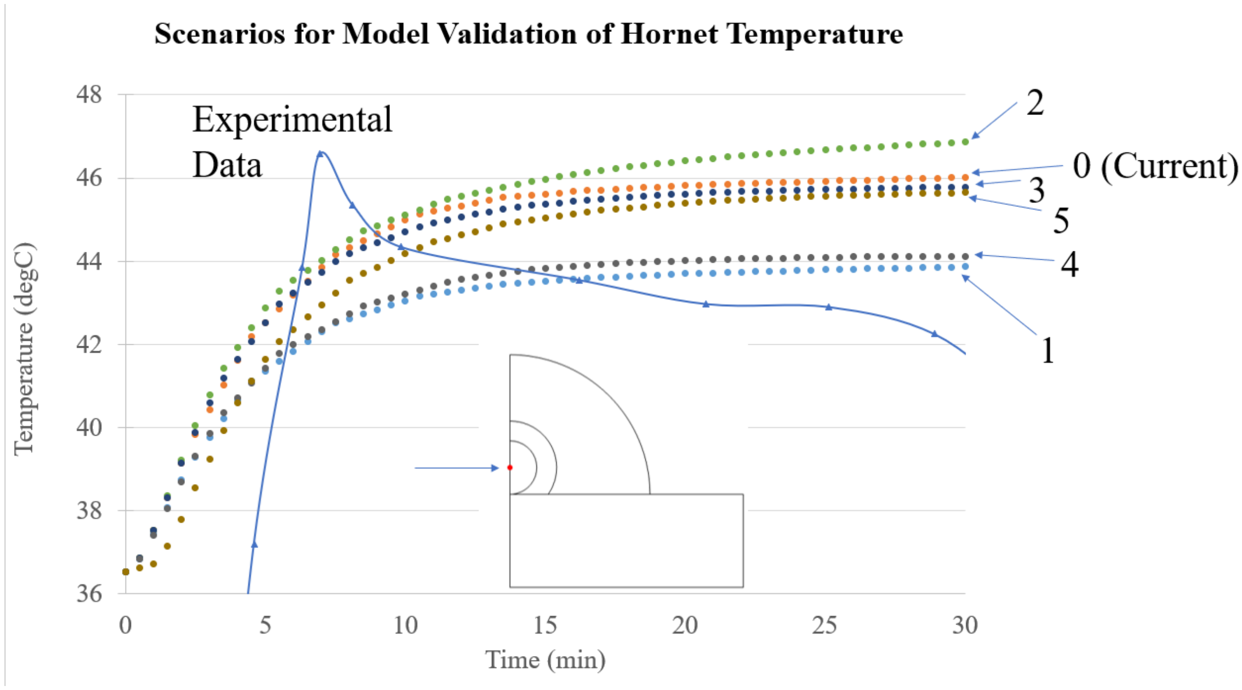

Figure 10: Hornet thoracic temperature validation as compared to literature data under different scenarios.

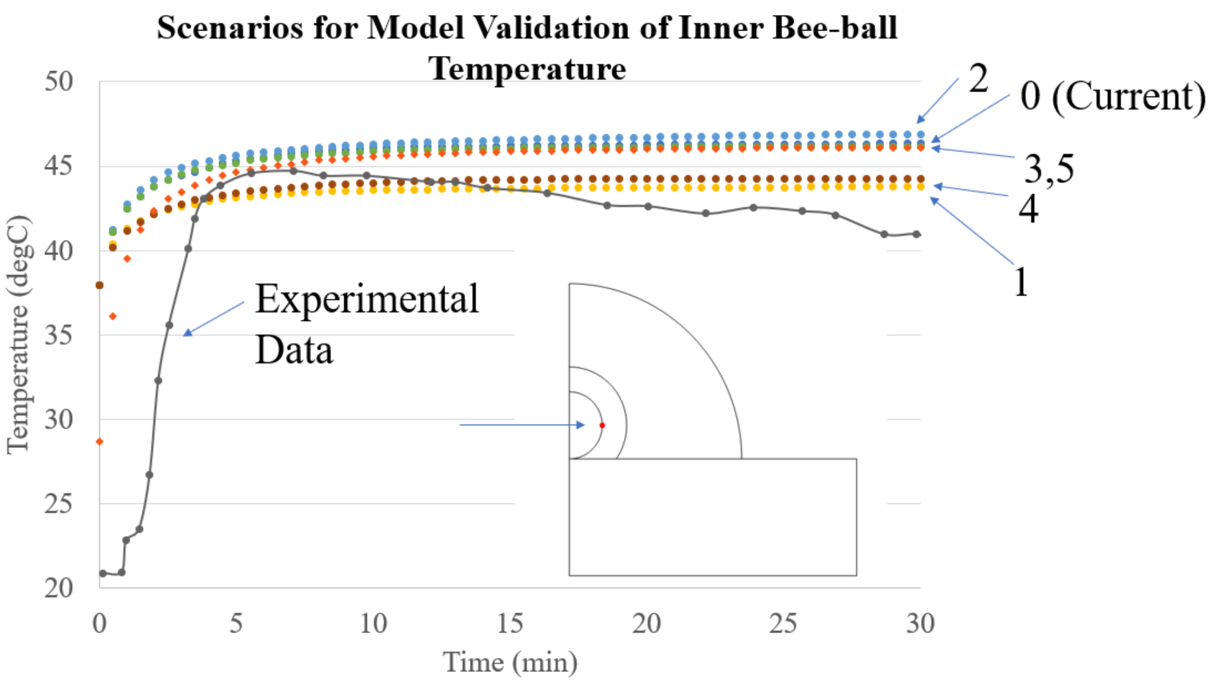

Figure 11: Honeybee internal temperature validation as compared to literature data under different scenarios.

None of the scenarios produced the decrease in temperature during the heat retaining phase nor did we observe the spike in hornet temperature at the end of the heating phase as the experimental data showed. This illustrates that some aspects of the process remain elusive from our formulation or may have been neglected in our assumptions. One such assumption is the constant size of the bee-ball throughout the entire time period. Observational studies of bee-balls note that some bees will disband the bee-ball prior to the breakup phase, thus shrinking the size of the bee-ball occurs especially towards the end of the heat retaining phase (Hosono et al. 2017). This may explain the gradual decrease throughout this phase.

6.2 CO_2 Transfer Validation

6.1.1 Validation with Experimental Data

To validate our experimental model, we compared the CO_2 profile of the bee-ball during the bee-balling process from our computational model to data provided in Sugahara & Sakamoto (2009). However, Sugahara & Sakamoto's experiment, different from our set up, two hornets were presented to the bee-carpet and the bee-ball is also at a significantly greater size (as shown in Figure A1 in the appendix). The CO_2 validation graph showed a pretty big inconsistency after 2 mins with our model approaching a steady state but the experimental data fluctuated up and down significantly.

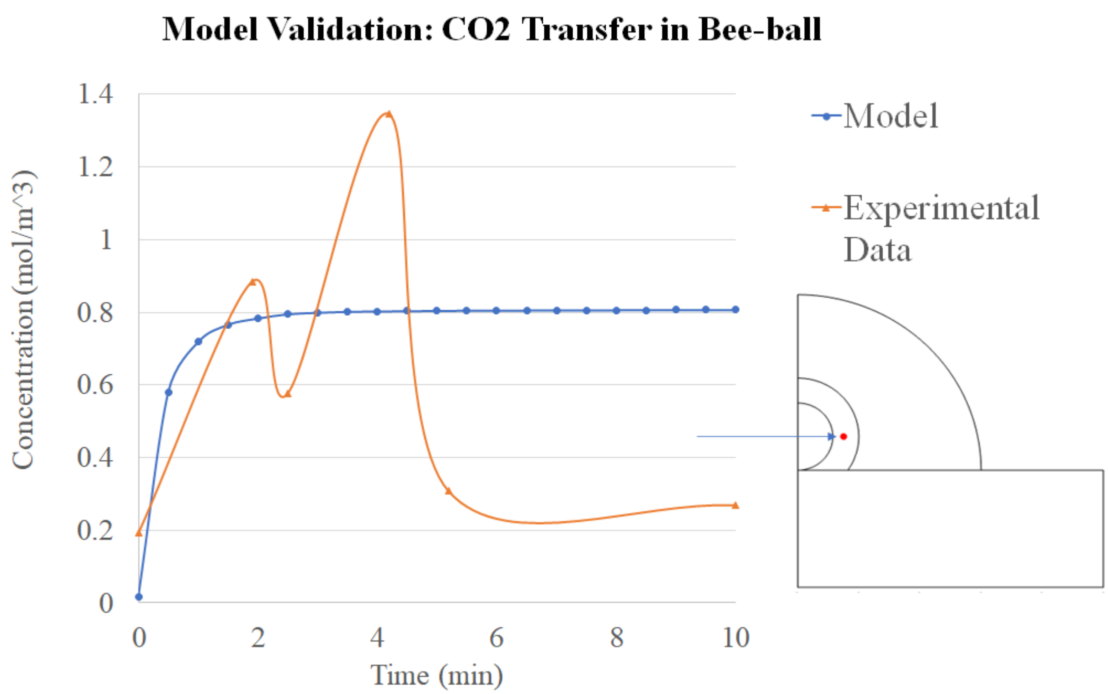

Figure 12: validation for CO_2 transport at the internal bee layer (above hornet surface) at point (0.0075, 0.00575)

In the modeling data, max CO_2 concentration is around 0.8 mol/m^3 whereas in literature the max CO_2 concentration is 1.3 mol/m^3. To quantify the difference between max CO_2 concentration and the experimental value, Equation 3 for percent difference is used.

$$\%\, difference = \frac{|V_1 - V_2|}{\frac{V_1 + V_2}{2}} \times 100 \tag{3}$$

V_1 = max CO_2 concentration from model and V_1 = 0.8 mol/m^3, V_2 = max CO_2 concentration from experimental data and V_2 = 1.3 mol/m^3. The percent difference was determined to be 47.62%.

6.1.2 The Effect of A Different Scenario on CO_2 Transfer

Similar to the validation for the heat transfer model there were inherent differences between the condition under which the experimental data was obtained and the conditions of a natural bee-ball that our model is run under. In the study of Sugahara & Sakamoto (2009), 2 hornets were presented to the bee-carpet and the bee-balling size is correspondingly a lot larger, whereas in our model, only 1 hornet is presented and the bee-ball size is correspondingly smaller (due to the lack of information in literature, this is by far the best data we could find). Hence, the actual experimental data we want to compare our modeling data to should be smaller than 1.3 mol/m^3 and the percent difference should be a little smaller than 47.62%. Another hypothesis for the difference is related to the break for biological CO_2 productions during the middle shown in Figure 12(around 2min) and dramatically decreases after 4 minutes. Without the break around 2 minutes, we expect to see it reach the highest level of CO_2 earlier.

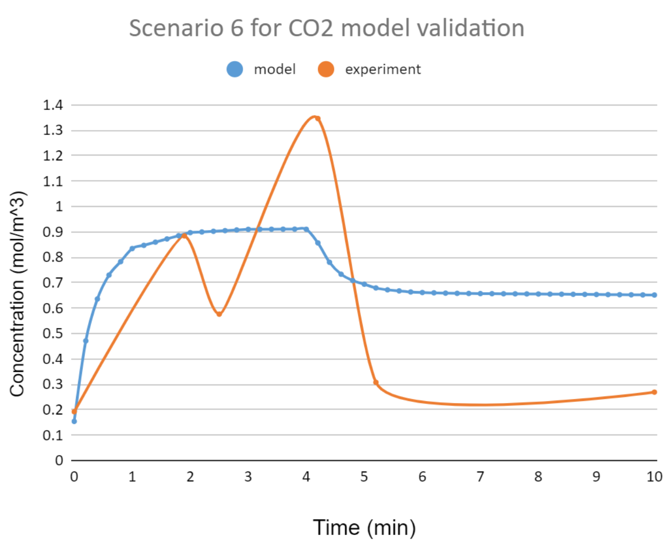

Figure 13. Scenario 6 for CO_2 of the hornet surface at pt (0.0075,0.00575) for model validation

To explore the presumption, here scenario 6 (Table 1), assuming after 4 min, the bee-ball reaches its maximum CO_2 concentration as well the highest temperature (45°C), the honeybees return to its normal CO_2 production rate under 30°C (approximately half of its CO_2 production rate under max temperature) and the hornet's CO_2 production is neglected assuming it has been killed. As shown in Figure 13, the concentration shows the decreasing trend after 4 min.

7 Sensitivity Analysis

To assess the dependence of the heat transfer and CO_2 transport model on the specific parameter values, we performed sensitivity analyses. The percent difference between the current results and results obtained when either: the parameters were increased 10% above and decreased 10% below or over a range .

For our sensitivity analysis of our heat model, we examined temperature variation at two specific points: the hornet center and the hornet/honeybee interface. With respect to the CO2 transport model we examined variation in CO_2 concentration at the surface of the hornet. Point study locations are illustrated in Figure 14:

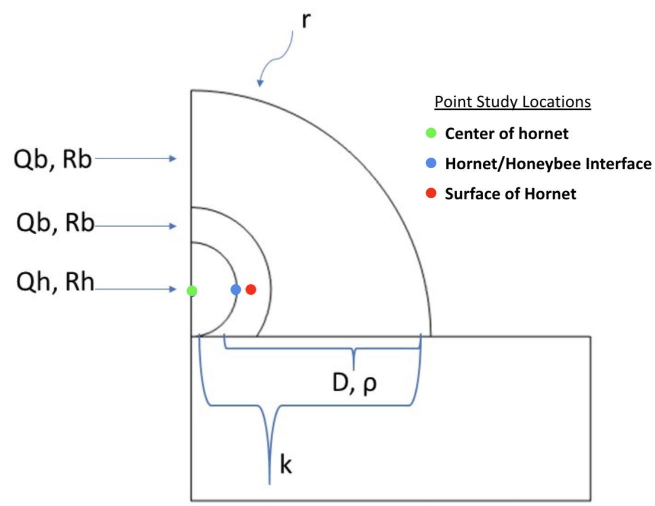

Figure 14: Schematic illustrating the point at which sensitivity analyses were conducted. The green dot locates at the center of the hornet at point (0, 0.00575); the blue dot locates at the hornet/honeybee interface at point (0.00575, 0.00575); and the red dot locates at the surface of the hornet at point (0.0075,0.00575).

With respect to the temporal point we chose 10 minutes. The 10 minute mark is a point of particular interest because in nature we would expect the peak temperature to occur around this time, variation here would have impliciation with regards to the success of the bee-ball in eliminating the hornet. For our sensitivity analysis of CO_2 transfer, we examined the variation in CO_2 concentration at a point just outside the hornet region, presumably in the air space that it would inhale. With respect to time, we selected the 4 minute mark given we would expect the CO_2 concentration to peak around this time (Sugahara & Sakamoto, 2009). The graphs below show the percent change in the generated numerical solution when the parameter was changed to the most extreme value within the range of possible data points.

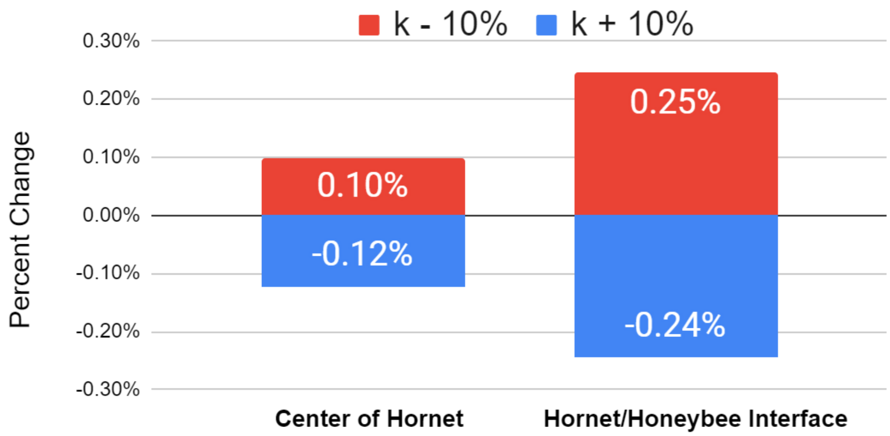

Figure 15: Sensitivity analysis for heat conductivity at 0.066 W/(m*K) and 0.054 W/(m*K) compare to conductivity at 0.06 W/(m*K). Temperature variation assessed at hornet center and hornet/bee interface at t = 10 minutes.

When the heat conductivity was increased by 10% and in the opposing direction reduced by 10%, the resulting temperature changed at both the hornet center and the hornet/honeybee interface was significantly under 1%. This suggests that the heat conductivity is not a major driving factor in the bee-balling process.

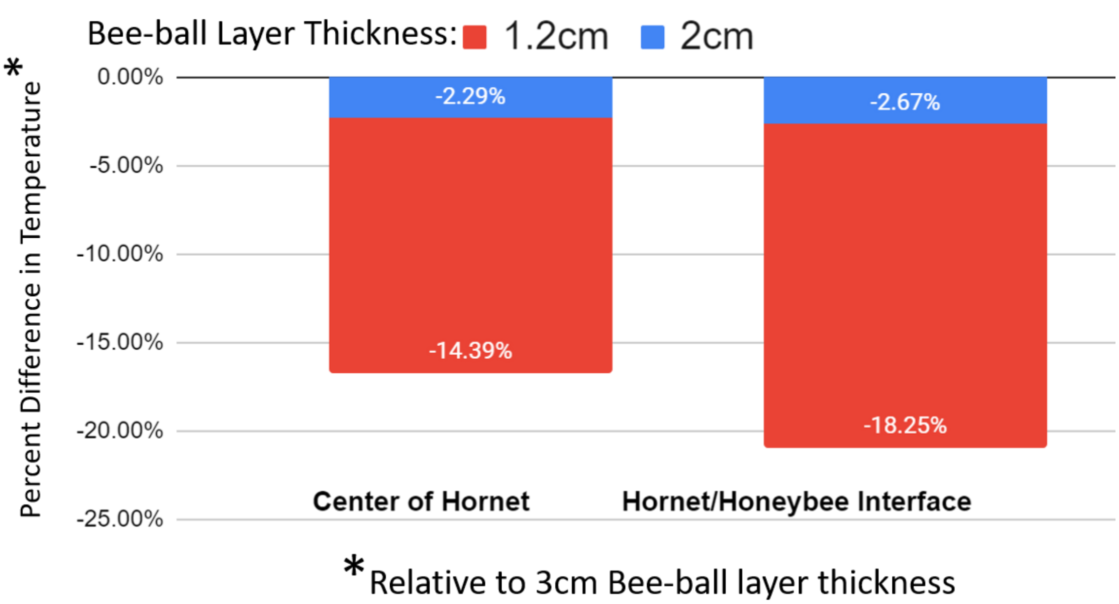

Figure 16: Sensitivity analysis for honeybee layer radius at 1.2 cm and 2 cm compared to radius of 3 cm by varying the thickness of the honeybee layer, while hornet size was held constant. Temperature variation assessed at hornet center and hornet/bee interface at t = 10 minutes.

From past research done by Sugahara et al, it is suggested that the bee-ball radius can vary from 1.2 - 3cm. Figure 16 shows that when honeybee layer thickness is decreased such that the total bee-ball radius shrinks from 3 cm to 1.2cm, there is a profound effect, 14.39% and 18.25% reduction in the temperature at the hornet center and the hornet/honeybee interface temperature respectively. When the honeybee layer thickness is decreased so that the total bee-ball radius decreases from 3 cm to 2 cm, we see a markedly smaller deviation from the model solution, a 2.29% and 2.67% reduction at the hornet center and hornet/honeybee interface respectively. This suggests that honeybee layer thickness, analogous to the number of participants in the bee-ball, plays a significant role below a certain threshold thickness. Interestingly while the results of our model suggest the initial temperature ramp during the heating phase of the bee-ball requires a minimum amount of participants, in nature successful bee-balls (success in terms of ability to reach lethal temperatures within the 10 minute period) may vary greatly in the number - some studies have observed bee-balls containing as few as 30 participants while others reported over 500.

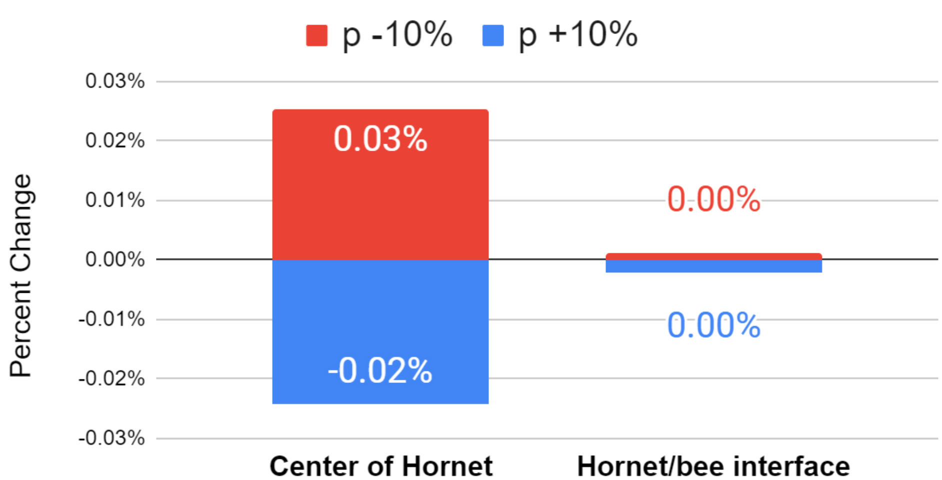

Figure 17: Sensitivity analyses of bee layer density by incrementing the parameter value 10% and reducing by 10%. Temperature variation assessed at hornet center and hornet/bee interface at t = 10 minutes.

Bee packing is characterized in part by density and also by extension, density dependent thermal conductivity. Given the nature of a bee-ball, both of these parameters are not easily nor directly measurable parameters experimentally while the bee-balling behavior is simultaneously occurring. Furthermore, there is little that can be done to manipulate this parameter to see its effect. With our model, however, we were able to vary the parameter value in this sensitivity analysis. From the results of our analysis, we observe that density exerts less than 1% reduction on the overall temperature when increased or decreased by 10%. Additionally, although not pictured here, we determined when the value was further decreased by 50% the percent difference remained under 1%.

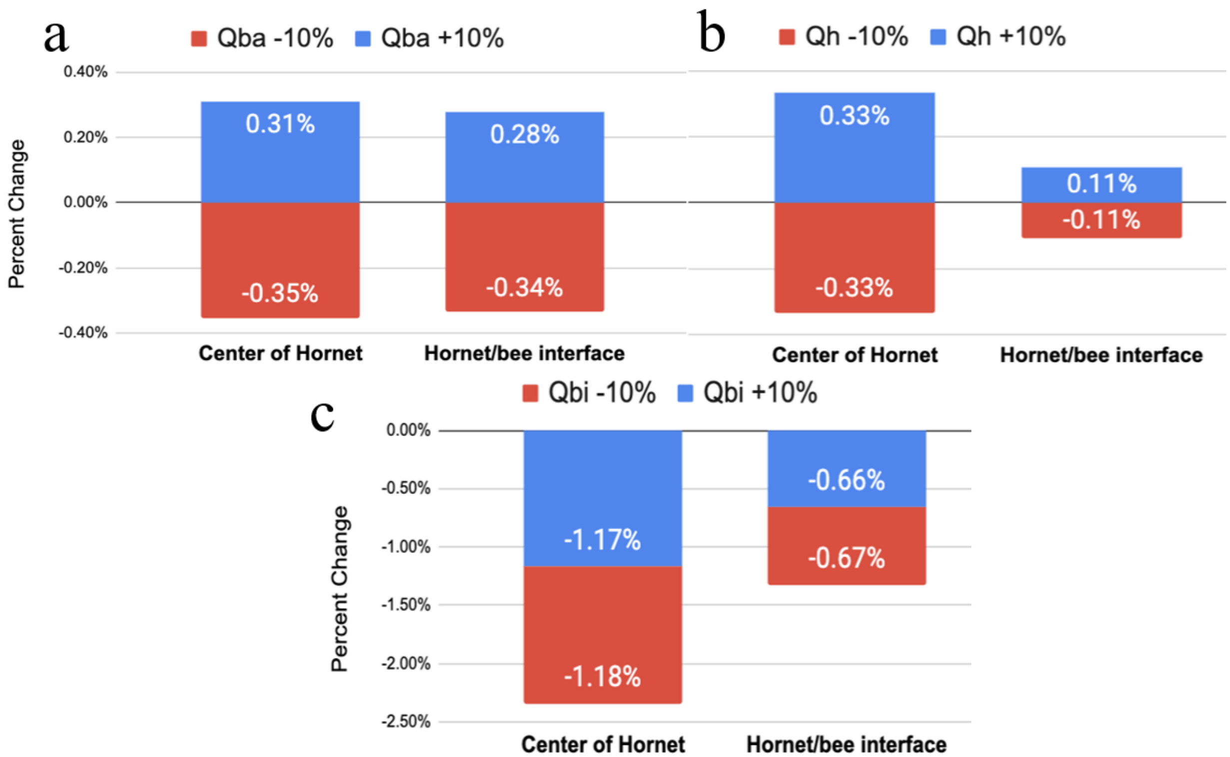

Figure 18: Sensitivity analysis of heat production by incrementing parameter value 10% (blue) and reducing 10% (red) for (a) active bee layer heat production rate (b)hornet heat production rate (c) inactive bee layer heat production rate;. Overall minimal temperature variation assessed at hornet center and hornet/bee interface at t = 10 minutes.

Manipulation of the heat production rates by 10% increments above and below the parameter values for the hornet and active bee layer's heat production produced minimal temperature variation. For both, the variation produced was less than 40% in the same direction as the change. Interestingly the manipulation of the heat production in the inactive bee layer's heat production layer we found that the variation caused did not produce variation in the same direction as the change. In both cases, the reduction and increase, a lower temperature was achieved at this specific point and time, unlike the trend in variation observed in the other two heat production. Similar to the other changes in heat production of the other regions, the overall variation was minimal after manipulation of 10%.

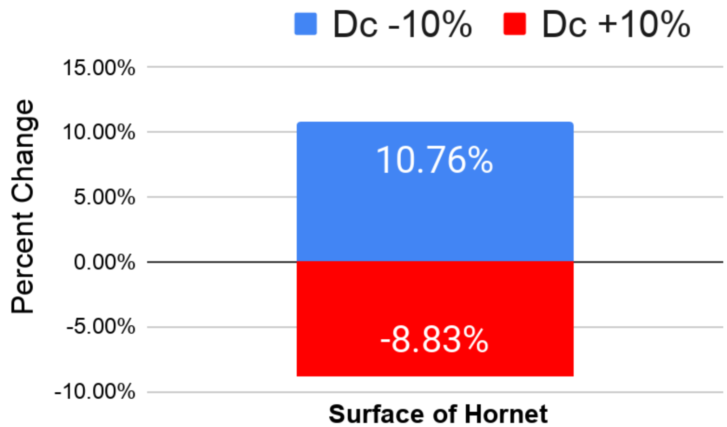

Figure 19: Sensitivity analysis of CO_2 diffusion coefficient (Dc) in beelayer by incrementation of the parameter value 10% (red) and reduction 10% (blue) at the surface of hornet, point (0.0075,0.00575), at t = 4 minutes.

When the CO_2 diffusion coefficient in honeybee layers was decreased by 10%, CO_2 concentration nearby the hornets spiracles was increased by 10.76%; while on the other hand, if the CO_2 diffusion coefficient in honeybee layers is increased by 10%, CO_2 concentration at the surface of the hornet decreases by 8.83%. This suggests that CO_2 diffusion coefficient in the honeybee layer exerts significant influence over the CO_2. Given that the diffusivity coefficient was calculated as an effective value dependent on the porosity of the honeybee layer unsurprisingly a less tightly packed bee-ball (a higher diffusivity) is more leaky, causing a reduction in CO_2.

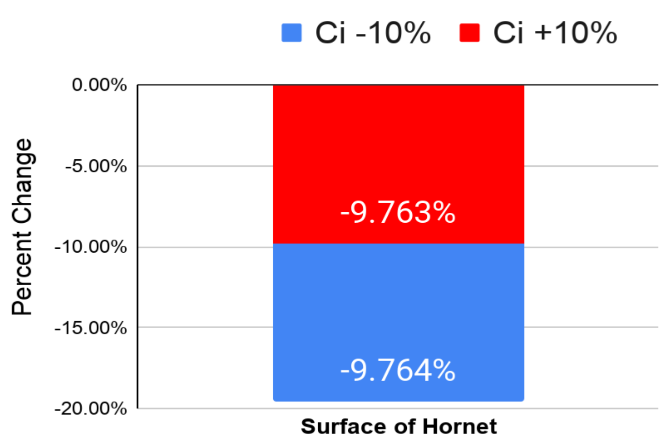

Figure 20: Sensitivity analysis of initial CO_2 concentration in beelayer by incrementation of the parameter value 10% (red) and reduction 10% (blue) at the surface of the hornet, point (0.0075,0.00575), at t = 4 minutes.

The initial CO_2 concentration in beelayer is set as CO_2 concentration in the air. Increasing and decreasing the initial CO_2 concentration by 10% both causes CO_2 concentration to decrease by 9.76% on the surface of the hornet at 4 minutes. This shows that the initial CO_2 concentration among the air in the bee-ball is a large factor affecting CO_2 concentration at peak.

8 Conclusion

Through analysis of the effect of different parameters, it is learned that varying values of the honeybee layer thickness, initial CO_2 concentration and CO_2 diffusivity had a substantial effect on the bee-balling process while other factors including heat conductivity, bee-ball density, heat & CO_2 production rate only had minimal effects. All this data provides researchers with the reasoning behind why bee-balls form, how the honeybees utilized heat and CO_2 production to effectively overheat and asphyxiate the hornet, and how honeybees modulate their movement, heat and CO_2 production rate to avoid overheating themselves. These conclusions combined with the sensitivity analysis to provide further insights into how varying parameter values and different natural conditions affect the bee-balling behavior in achieving the max temperature to kill the hornet.

However, given the lack of previous research on the bee-balling process, many heat and CO_2 transfer parameters used in this model were gathered from different literatures where experiment setting may not be 100% consistent; many parameters also relied on our assumptions and calculations. Hence, the final results produced in this model may not resemble reality that well due to limitations in reliable parameter values we can find. In addition, there might be some biological mechanisms that's unknown, which have not been reported in previous studies either, that resulted in some of the discrepancies we observed in experimental data and computational solutions. All these uncertainties can prompt future research and experiment on the bee-balling process.

9 Discussion

Results of the model also provide insights as to why European honeybees are generally unsuccessful in bee-balling compared to Japanese honeybees, *Apis cerana*. Results of previous experimental studies have elucidated that bee-balls formed by Japanese honeybees, kill Asian Giant Hornets, through exposure to excessive thermal stress. However, experiment alone fails to identify the specific key features of the *Apis cerana* bee-ball that permit its consistent success while its European relative, *Apis mellifera,* more frequently fails to mount a successful defense.

Although both *Apis mellifera* and *Apis cerana* are of the same species anatomically, they do differ slightly with respect to chiefly size, weight and relative hairiness. In bee-ball formation, these discrepancies in size, weight, hairiness and other aspects of the bees are effectively captured in the density, thermal conductivity and specific heat of the bee regions. Our findings demonstrate that manipulation of these parameters produces minimal temperature variation which suggest that the bee-balls ability to reach lethal temperature at its peak is independent of anatomical differences between species. Furthermore, both *Apis mellifera* and *Apis cerana* expected to have similar heat generation potentials (the same magnitude of heat generation in both passive and active heating), given both participate in overwintering clusters and require preflight warm up of their muscles. In addition, our findings also illustrate that manipulation of Q produces little variation in temperature. In all, this goes to invalidate the notion that european honeybees are physically incapable of producing a successful bee-ball and strongly suggest behavioral differences as the differentiating factor between the species rate of success. This finding further corroborates the work by Ugajin et al. (2012) whose experiments detected increased neural activity in Japanese honeybees associated with thermal stimuli processing at bee-ball temperatures (46°C), suggesting that behavior is the key delimiter of successful bee-balls.

Extending the findings of this study may also help inform more environmentally friendly pest control. Bee-ball in a sense could be viewed as a living insect trap that the bees use to eliminate a troublesome pest. First, they attract the hornet (unintentionally), then they restrain, then heat and CO_2 is produced to a level exceeding the pests critical limit. The bees are limited by their own material properties and need to remain alive however a non-living trap is not. We propose a bee-ball trap composed of two materials, the inner material that upon the application of force releases heat and a highly insulative and low diffusivity outer material. By adding an attractant and adhesive to the trap interior to lure the hornet and prevent it from escaping, the trap could function similar to that of a bee-ball. Using heat and CO_2 accumulation from the hornet itself in a reusable trap instead of pesticides one could avoid potential health and environmental risks and lower costs associated with pest management.

10 Appendix

10.1 Model Parameters

Table A1:

List of parameters and their values, with sources and calculation procedures.

HoneyBee	**Expression**	**Source and Notes**
Thermal Conductivity: kb	0.20 [W/(m*K)]	Basak et al., 1996
Specific Heat Capacity: cpb	1422.5 [J/(kg*K)]	Basak et al., 1996 Using Average of: 1280, 1850, 1110, 1450, 1422.5 corresponds with $\epsilon = 0.72$ ($\rho_b = \frac{m_b}{V_b} = 1.48 mg/mm^3$, m_b = mass of a bee=115mg,$V_b$volume of bee =77.75m^3 approximating body shape as a cylinder $\hat{c}_{pb}$= 3500J kg^{-1} K^{-1},) $c_p = (1 - \epsilon)\rho_b \hat{c}_{pb}$
Heat Production Rate: Qb	Active Bees = 2.9e5 W/m^3 Passive Bees = 1000 W/m^3 See Figure A3	Humphrey & Dykes, 2008 Bee's metabolic rate is temperature dependent, however data of metabolic rates at high temperatures can't be found. Given the core region bees are the primary source of heat in a bee-ball with active metabolism, and honeybees of high activity display a linear decrease in heat production with increasing temperature, we generated the following interpolation using the rates of heat production found for active and passive bees(see figure A3). This interpolation represents the most drastic modification expected to occur from completely active metabolism initially to entirely passive metabolism at peak temperature.We assumed the primary function of outside bees are to insulate and maintain a constant passive rate of heat production.
Density of bee-ball: pb	360g/L	Omholt, 1987 density at center of bee-ball = 1.25 bees/ml; on the outer side= 5.5 bees/ml; taking the average ~ 3 bees/ml; taking weight of a bee = 120mg/bee; density = 360mg/ml = 360g/L
Depth of bee layer: d	Outer radius of bee-ball= 4-6cm	Sugahara et al., 2012

Initial Bee Temperature: T0b	39.55 C	Stabentheiner et al., 2012
Rate of CO_2 Production: vb	See Figure A5	Kovac et al., 2007 resting/'exothermic' CO_2 respiration rates are assumed for active/'endothermic' bees.
Diffusivity of CO_2: dif_bee	linear interpolation: 23.9C, Deff = 7.6453e-6 m^2/s 22.2C, Deff = 7.6453e-6 m^2/s 21.7C, Deff = 7.535e-6 m^2/s 20.7C, Deff = 7.755e-6 m^2/s 20.1C, Deff = 7.755e-6 m^2/s	Prichard & Currie, 1982 interpolation provided in literature was used to calculate the effective diffusivity for the bee-ball. A factor of 0.55 representing the average ratio of air in a bee-ball was used in the calculation
# of bees	100-500	Hosono et al., 2017

Hornet	**Expression**	**Source and Notes**
Thermal Conductivity: kh	K = 0.15 - 0.25 W/mK	Basak et al., 1996 Assumed to be same as honeybee (neglects effect of cuticle)
Specific Heat Capacity: cph	3500[J/(kg*K)]	Basak et al., 1996 Assumed to be same as honeybee (neglects effect of cuticle)
Density: ρh	301 kg/m^3	Matsuura & Sakagami Hornet weight=1.25g, diameter=1.15cm, length=4cm. Assuming the hornet to be a cylinder
Rate of Heat Production: Qh	At 26C , Q = 6923W/m^3 At 23C, Q = 8036.7W/m^3	Schmolz et al.,1999
Initial Temperature:Thi	32-34 °C	Stabentheiner et al., 2012
Rate of CO_2 Production: vh	As illustrated in Figure A4	Kafer et al., 2012 resting/'exothermic' CO_2 respiration rates are assumed for hornets
Hornet diameter	1.15cm	Matsuura & Sakagami Diameter = head width
Hornet length	4cm	Sugahara et al., 2012

Honeybee Comb	**Expression**	**Source and Notes**
Assuming the comb is filled with honey. Considering for every 8 pounds of total weight, 1 pound of comb and 7 pounds of honey. v_{honey}=7kg/1400kg*m^3, $v_{comb\ wax\ wall}$=1kg/950kg*m^3 , v_{honey}: $v_{comb\ wax\ wall}$=4.75		

Hence, for a comb full of honey, there is 82.6% v_{honey}, 17.4% $v_{wax\ wall}$, then using parameters given in literature for honey and air properties from Humphrey et al., (2008) kc, cpc, and ρc are calculated as described below.		
Thermal Conductivity: kc	0.5652[W/m/K]	Humphrey et al., 2008 $K_c = 82.6\%*K_{honey}+17.4\%*K_{wax\ wall} =0.826 * 0.60 + 0.174 * 0.40 = 0.5652$
Specific Heat Capacity: cpc	2334.8J/(kgK)	Humphrey et al., 2008 $C_p = 0.826\ C_{p\ honey} * 0.174C_{p\ wax\ wall} = 0.826 * 2300 + 0.174 * 2500 = 2334.8$
Initial Temperature: Ti	34.5	32 - 35°C is optimal temperature to store honey
Diffusivity of CO_2: dif_comb	3.99 x 10^-7 m^2 /s.	Murrell et al.
Density: ρc	1321.7kg/m^3	Humphrey et al., 2008 $\rho c=0.826\rho_{honey}+0.174\rho_{wall} =0.826*1400 + 0.174*950 = 1321.7$

Air	**Expression**	**Source and Notes**
Ambient Temperature: T∞	T∞ = 32.75 C	Average autumn temperature in Japan, peak hornet hunting season, corresponding to most frequent bee-balling
Initial CO_2 concentration in hives	0.4% =0.153mol/m^3	Seeley, 1974 Average concentration
Constant boundary CO_2 concentration in comb: cc	2.69e-4mol/L =0.269mol/m^3	Sugahara et al., 2012 "The CO_2 level in a normal bee space of the open nest was measured as 0.7%." 0.007/26mol/l=2.69e-4mol/L
Convective heat transport coefficient: h	h = 10 (W/m^2C)	Phillip et al., 2013 Under free air convection, the convective coef is around 2.5-25 W/m^2C, we are taking value in the middle for 10 W/m^2C
Diffusivity of CO_2: dif_air	D_{co_2} = 1.6e-5 m^2/s	Sudarsan et al., 2012
CO_2 bulk concentration in air: $c_{b,c}$	c_{air} = 0.0155 mol/m^3	Engineering Toolbox, 2019 CO_2 = 410 ppm in 2018 Conversion: 795 mg/m^3= 795e-3g/m^3 (795e-3g/m^3)/(44g/mol)=0.01807mol/m^3

10.2 Relevant Figures

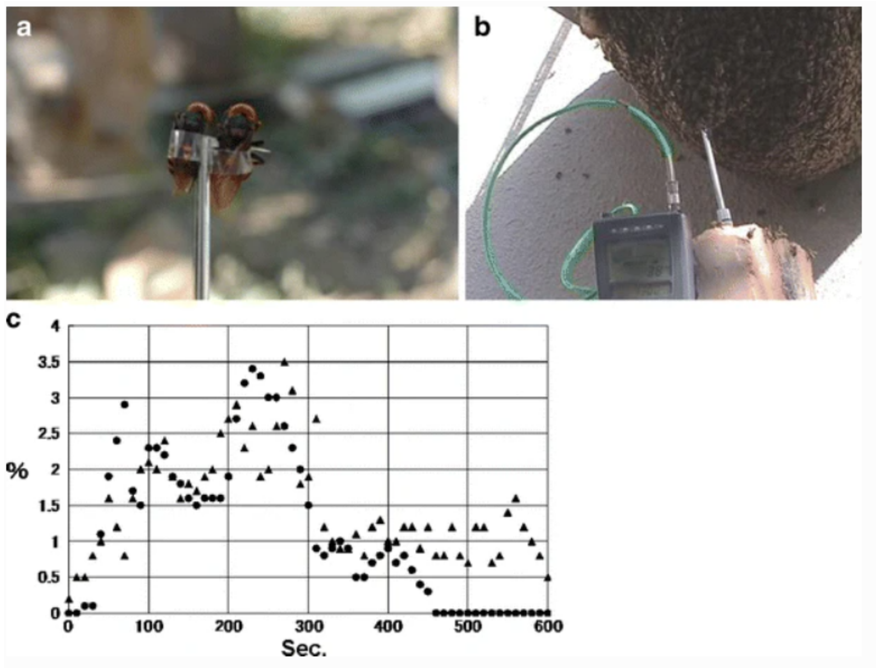

Figure A1: **a**. Two hornets were introduced into the tip of the gas detector. **b**. The CO_2 level was measured within the bee-ball beneath the open nest. **c**. CO_2 levels inside bee-balls (two cases) at 10-s intervals. Features during the initial 5 min and the latter half changed markedly.

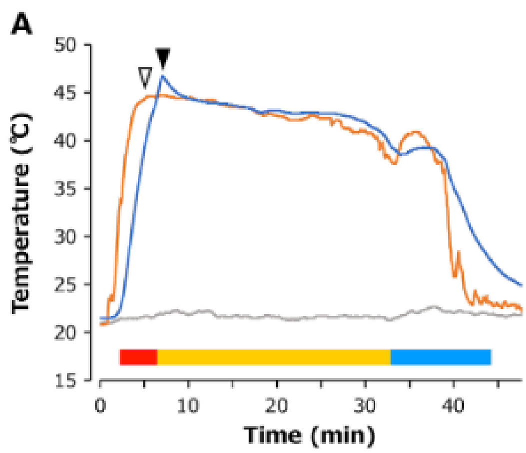

Figure A2: Experimental data from Hosono et al. (2017). Entire temperature (℃) changes during bee‐balling behavior vs time (min). The orange line represents the honeybee temperature profile and the blue line represents the hornet temperature profile. Three phases of bee‐ball temperature are shown with color bars: heating phase (red), heat‐retaining phase (yellow) and break‐up phase (blue).

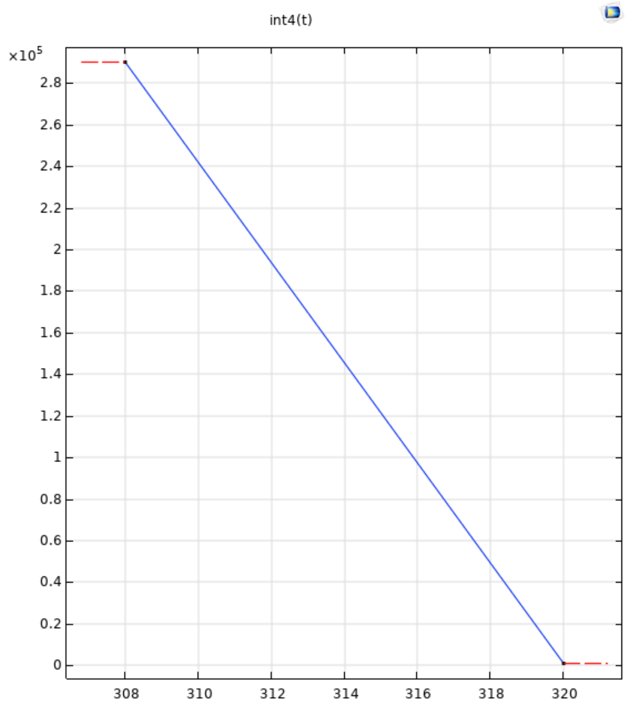

Figure A3: Metabolic Heat interpolation used for the core bee region of the domain

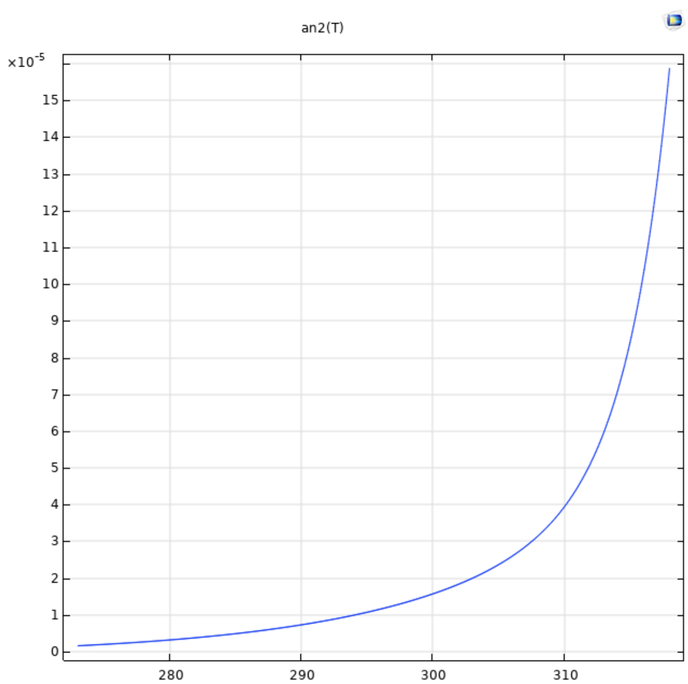

Figure A4: Hornet CO_2 Production Rate expression: ((9.7023e-5*exp((T-273)/3.11195))+(4.63097*exp((T-273)/14.6382))+(56769.01521*exp ((T-273)/ 3.81259e84))-56770.80269)*5.603e-7

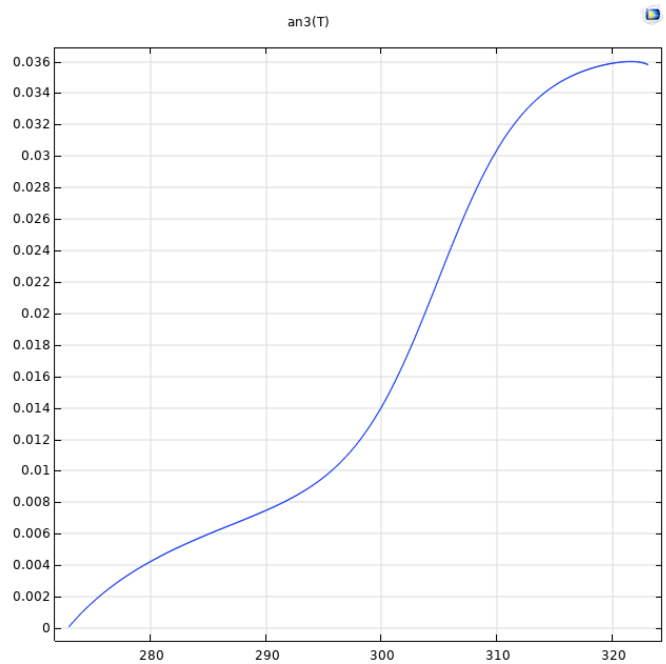

Figure A5: Bee CO_2 Production Rate expression: ((47.7497+(45.4819/(1+exp(8.6047-(0.26935*(T-273))))))+(exp(1)/((T-273)-51.8))-(exp(1)/(.02268*log((T-273)+12.4505))))*5.74e-4

9.3 CPU Time

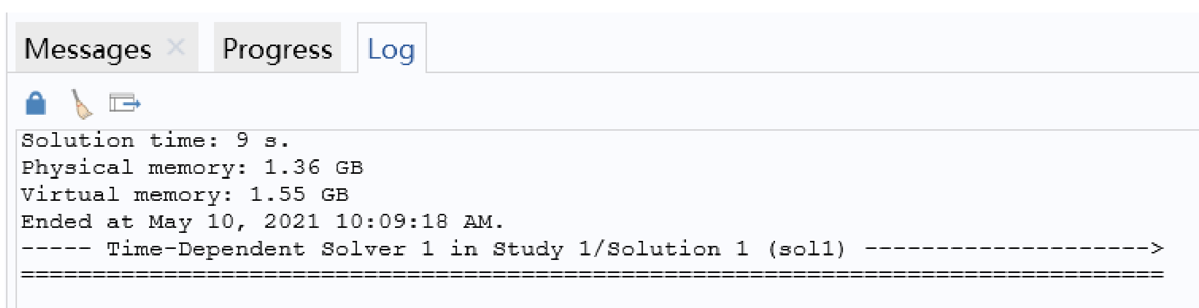

Figure A6: For a typical run, the solution time is 9 seconds, the physical memory being used is 1.36 GB and the virtual memory being used is 1.55 GB.

11 References

Bahreini, R., & Currie, R. W. (2015). The Potential of Bee-Generated Carbon Dioxide for Control of Varroa Mite (Mesostigmata: Varroidae) in Indoor Overwintering Honey Bee (Hymenoptera: Apidae) Colonies. *Journal of Economic Entomology*, *108*(5), 2153–2167. https://doi.org/10.1093/jee/tov202

Basak, T., Rao, K. K., & Bejan, A. (1996). A model for heat transfer in a honey bee swarm. *Chemical Engineering Science*, *51*(3), 387–400. https://doi.org/10.1016/0009-2509(95)00283-9

Datta, A. (2017). *Heat and Mass Transfer : A Biological Context.* CRC Press LLC.

Heinrich, B. (1979). Thermoregulation of African and European Honeybees During Foraging, Attack, and Hive Exits and Returns. *Journal of Experimental Biology*, *80*(JUN), 217–229.

Hosono, S., Nakamura, J., & Ono, M. (2017). European honeybee defense against Japanese yellow hornet using heat generation by bee-balling behavior. *Entomological Science*, *20*(1), 163–167. https://doi.org/10.1111/ens.12248

Humphrey, J. A. C., & Dykes, E. S. (2008). Thermal energy conduction in a honey bee comb due to cell-heating bees. *Journal of Theoretical Biology*, *250*(1), 194–208. https://doi.org/10.1016/j.jtbi.2007.09.026

Käfer, H., Kovac, H., & Stabentheiner, A. (2012b). Resting metabolism and critical thermal maxima of vespine wasps (Vespula sp.). *Journal of Insect Physiology*, *58*(5), 679–689. https://doi.org/10.1016/j.jinsphys.2012.01.015

Kovac, H., Stabentheiner, A., Hetz, S. K., Petz, M., & Crailsheim, K. (2007). Respiration of resting honeybees. *Journal of Insect Physiology*, *53*(12), 1250–1261. https://doi.org/10.1016/j.jinsphys.2007.06.019

Lemke, M., & Lamprecht, I. (1990). A Model for Heat-Production and Thermoregulation in Winter Clusters of Honey Bees Using Differential Heat-Conduction Equations. *Journal of Theoretical Biology*, *142*(2), 261–273. https://doi.org/10.1016/S0022-5193(05)80227-9

Matsuura, M., & Sakagami, S. (1973). A Bionomic Sketch of the Giant Hornet, Vespa mandarinia, a Serious Pest for Japanese Apiculture.

Nouvian, M., Reinhard, J., & Giurfa, M. (2016). The defensive response of the honeybee *Apis mellifera*. *The Journal of Experimental Biology*, *219*(22), 3505–3517. https://doi.org/10.1242/jeb.143016

Omholt, S. W. (1987). Thermoregulation in the winter cluster of the honeybee, Apis Mellifera. *Journal of Theoretical Biology*, *128*(2), 219–231. https://doi.org/10.1016/S0022-5193(87)80170-4

Ono, M., Okada, I., & Sasaki, M. (1987). Heat-Production by Balling in the Japanese Honeybee, Apis-Cerana-Japonica as a Defensive Behavior Against the Hornet, Vespa-Simillima-Xanthoptera (hymenoptera, Vespidae). *Experientia*, *43*(9), 1031–1032.

https://doi.org/10.1007/BF01952231
Schmolz, E., Brüders, N., Schricker, B., & Lamprecht, I. (1999). Direct calorimetric measurement of heat production rates in flying hornets (Vespa crabro; Hymenoptera). *Thermochimica Acta*, *328*(1), 3–8. https://doi.org/10.1016/S0040-6031(98)00617-0
Southwick, E.E. (1985). Thermal conductivity of wax comb and its effect on heat balance in colonial honey bees (Apis mellifera L.). Experientia 41, 1486–1487. https://doi-org.proxy.library.cornell.edu/10.1007/BF01950051
Stabentheiner, A., Kovac, H., & Schmaranzer, S. (2007). Thermal Behaviour of Honeybees During Aggressive Interactions. *Ethology*, *113*(10), 995–1006. https://doi.org/10.1111/j.1439-0310.2007.01403.x
Sudarsan, R., Thompson, C., Kevan, P. G., & Eberl, H. J. (2012). Flow currents and ventilation in Langstroth beehives due to brood thermoregulation efforts of honeybees. *Journal of Theoretical Biology*, *295*, 168–193. https://doi.org/10.1016/j.jtbi.2011.11.007
Sugahara, M., Nishimura, Y., & Sakamoto, F. (2012). Differences in Heat Sensitivity between Japanese Honeybees and Hornets Under High Carbon Dioxide and Humidity Conditions Inside bee-balls. *Zoological Science*, *29*(1), 30–36. https://doi.org/10.2108/zsj.29.30
Sugahara, M., Sakamoto, F. (2009). Heat and carbon dioxide generated by honeybees jointly act to kill hornets. *Naturwissenschaften 96*, 1133–1136. https://doi.org/10.1007/s00114-009-0575-0
Murrell, K. (2013). A STUDY OF CARBON DIOXIDE DIFFUSIVITY THROUGH SAND. *Oklahoma State University*, 1-45.
Seeley, T. (1974). Atmospheric carbon dioxide regulation in honey-bee (Apis mellifera) colonies. *Journal of Insect Physiology*, 2301-2305, https://doi.org/10.1016/0022-1910(74)90052-3.
Engineering ToolBox, (2019). Atmospheric Carbon Dioxide Concentration. https://www.engineeringtoolbox.com/atmospheric-carbon-dioxide-concentration-d_2169.html